IOP Publishing Journal of Physics: Condensed Matter
J. Phys.: Condens. Matter **29** (2017) 343002 (18pp) https://doi.org/10.1088/1361-648X/aa76c7

Topical Review

High resolution SPM imaging of organic molecules with functionalized tips

Pavel Jelínek

Institute of Physics, Czech Academy of Sciences, Cukrovarnická 10, 162 00, Prague, Czech Republic

E-mail: pavel.jelinek@fzu.cz

Received 3 September 2015, revised 31 May 2017
Accepted for publication 2 June 2017
Published 25 July 2017

Abstract

One of the most remarkable and exciting achievements in the field of scanning probe microscopy (SPM) in the last years is the unprecedented sub-molecular resolution of both atomic and electronic structures of single molecules deposited on solid state surfaces. Despite its youth, the technique has already brought many new possibilities to perform different kinds of measurements, which cannot be accomplished by other techniques. This opens new perspectives in advanced characterization of physical and chemical processes and properties of molecular structures on surfaces. Here, we discuss the history and recent progress of the high resolution imaging with a functionalized probe by means of atomic force microscopy (AFM), scanning tunnelling microscopy (STM) and inelastic electron tunneling spectroscopy (IETS). We describe the mechanisms responsible for the high-resolution AFM, STM and IETS–STM contrast. The complexity of this technique requires new theoretical approaches, where a relaxation of the functionalized probe is considered. We emphasise the similarities of the mechanism driving high-resolution SPM with other imaging methods. We also summarise briefly significant achievements and progress in different branches. Finally we provide brief perspectives and remaining challenges of the further refinement of these high-resolution methods.

Keywords: nc-AFM, STM, IETS, molecular structure, surface science, on-surface chemistry

(Some figures may appear in colour only in the online journal)

1. Introduction

The invention of STM [1] and AFM [2] more than 30 years ago were two significant milestones initiating the era of Nanoscience and Nanotechnology. The possibility to image and manipulate individual atoms or molecules on surfaces opened new perspectives for control and understanding of the physical and chemical processes at the atomic scale. While atomic resolution on different kinds of surfaces became routinely achieved, reaching at least a moderate spatial resolution on single molecules was very difficult. Usually molecules were only imaged as featureless objects lacking any signature of internal structure. Indeed the internal resolution of molecules on surfaces by means of SPM remained a great challenge for many years.

The situation has changed drastically with the discovery of enhanced molecular contrast using a proper tip functionalization a few years ago. The main obstacle to achieving sub-molecular contrast is a relatively weak signal-to-noise ratio detected during measurements. Thus, an important ingredient for achieving high-resolution imaging is proper decoration of the tip apex by an atom or molecule intentionally/accidentally picked up from the surface, which serves to significantly amplify the detected signal. The unprecedented sub-molecular resolution of organic molecules on solid state surfaces achieved under ultra high vacuum (UHV) by both STM and AFM modes represents one of the most remarkable and exciting achievements in the SPM field in the last years. The possibility to achieve detailed information about the chemical structure of a single molecule, *a priori* unknown, on surfaces

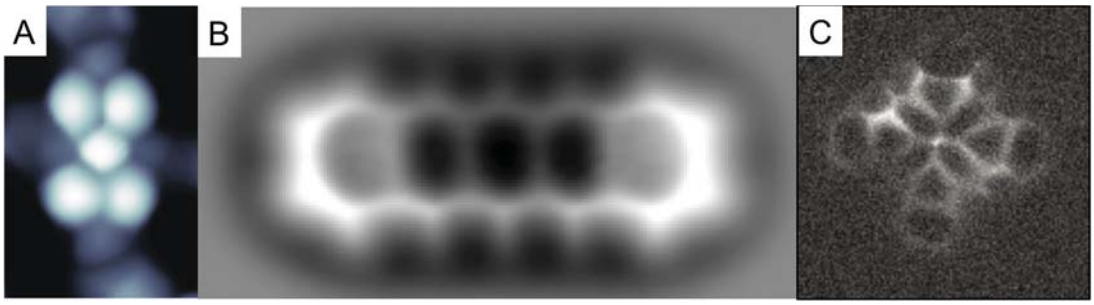

Figure 1. Examples of high resolution STM, AFM and IETS–STM images of molecules obtained with functionalized tips: (a) Experimental constant height HR-STM dI/dV figure of PTCDA/Au(1 1 1) obtained with CO-tip at $V_{bias} = -1.6$ V with respect to the sample. Reproduced from [15]. © IOP Publishing Ltd. All rights reserved. (b) Constant height nc AFM simulations of a pentacene molecule on Cu(1 1 1) surface acquired with CO-tip. From [18]. Reprinted with permission from AAAS. (c) constant-height IETS–STM image of CoPc molecule on Ag(1 1 0) surface with CO-tip (adopted from [32]). From [32]. Reprinted with permission from AAAS.

opens completely new possibilities in surface science, chemistry, biology and nanoscience.

Personally, I believe that the basic principles of the mechanism providing the high-resolution AFM/STM contrast (i.e. lateral relaxation of a frontier atom/molecule on tip apex) can be also applied to the understanding of atomic contrast observed on metal surfaces using electrochemical STM [3], and STM operating in the contact mode [4–6], or the recently observed atomic contrast of non-contact AFM in liquids [7, 8].

In this review, we will discuss the history, current understanding and some perspectives of high-resolution contrast and its applications going beyond simple imaging of the chemical structure of organic molecules on surfaces. We will describe details of the mechanism responsible for the unprecedented spatial sub-molecular resolution. We will emphasise similarities of the mechanism driving high-resolution SPM with other imaging methods. We will discuss what else we can learn from high-resolution SPM images beyond the molecular structure. Finally we will provide brief perspectives and outlook of the high-resolution methods.

Of course, it is not possible to provide the comprehensive review of the progress and all results achieved last years. Furthermore, the content of this review article, especially emphasis on certain aspects and results of the technique, is certainly biased by the personal view of the author. Thus to gather a more complex picture of the field, I also refer the reader to other overviews related to the field of high-resolution SPM imaging [9–12].

2. Brief history

Probably the first evidence of the contrast enhancement due tip functionalization was reported by Jascha Repp and his colleagues in 2005 [13]. In this seminal paper, they presented real space STM imaging of molecular orbitals of a pentacene molecule deposited on an insulator layer. They demonstrated that the contrast was significantly increased by the presence of a pentacene molecule located on the tip apex. The sharp contrast can be further enhanced by the selection rules governing the tunnelling process across the STM junction, as it was later explained theoretically [14] and/or lateral bending of the molecule on tip [48].

In 2008, Ruslan Temirov and his colleagues [15] discovered that an admission of hydrogen molecules into the UHV chamber induces the significant enhancement of molecular contrast observed in STM images when tip is brought very close to an inspected surface. The STM images contain characteristic sharp edges, which mimic very well the molecular structure of perylenetetracarboxylic dianhydride (PTCDA) molecules, see figure 1(a). They attributed this effect to the presence of the hydrogen molecules in the tunnelling junction preferentially bounded to a metallic tip apex. Afterwards, they demonstrated that a variety of other functionalized tips intentionally decorated by atoms (Xe) or molecules (CH_4, CO) also enable resolution of chemical structures of large organic molecules deposited on metallic surfaces with unprecedented details [16, 17]. For historical reasons, this technique is known as scanning tunneling hydrogen microscopy (STHM).

One year later, Leo Gross and his colleagues [18] published their seminal work presenting high-resolution AFM images of pentacene molecule, see figure 1(b), deposited on an insulating thin film and metallic surface employing so called non-contact (nc) AFM mode [19, 20]. The key step was a controlled functionalization of metallic tip apex with a single carbon monoxide (CO) molecule [21]. The high-resolution AFM images contain sharp edges revealing clearly the internal chemical structure of the molecule similarly to STHM technique. This discovery has stimulated research activities of many groups, namely in the community of nc-AFM [22], to achieve, understand and further explore this high-resolution imaging. This effort has brought significant advances not only in the characterisation of molecular structures on surfaces [23–26] but also in the understanding of chemical transformation on surfaces [24, 27, 28] or investigating weak van der Waals interactions [29–31].

Finally in 2014, Wilson Ho's group presented an alternative approach to achieve high-resolution contrast by employing IETS channel [32]. They mapped out variations of the IETS signal of the frustrated translational mode of CO molecule placed on the tip apex while scanning over molecules deposited on a metal surface. In close tip-sample distances, the IETS maps reveal sharp contrast mimicking the molecular structure, in very similar manner to those observed with AFM and STM, see figure 1(c). The similarity of the contrast

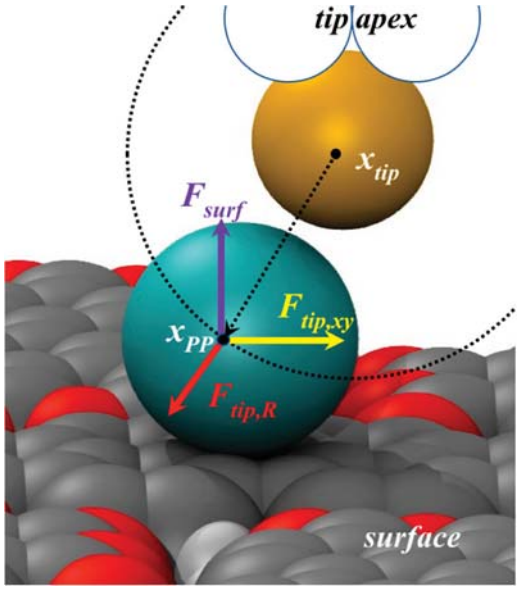

Figure 2. Schematic representation of forces acting on the probe particle representing the functionalized tip in the mechanistic PP-model: The probe particle (green ball) experiences different interactions from the surface F_{surf}, the tip apex $F_{tip,R}$ and lateral force $F_{tip,xy}$. Adapted with permission from [39], Copyrighted by the American Physical Society.

between different high-resolution modes indicates a common mechanism, which is responsible for the sub-molecular contrast [33].

Nowadays the basic mechanism of the high-resolution AFM images is fairly well understood. In their landmark paper [18], Gross and his colleagues attributed the origin of high-resolution AFM imaging to Pauli repulsion [34], which dominates the tip-sample interaction at close distances. Later Gross and Moll also pointed out the importance of a lateral bending of the functionalized tip apex [35]. This effect was further elaborated by others [36–40]. About the same time in 2014, two groups independently proposed similar mechanistic models [39, 40], which can explain the main ingredients of the AFM imaging mechanism. In the approach devised by Hapala *et al* [39], they introduced the concept of a so-called probe particle (PP) model, where a flexible molecule/atom located at the tip apex is represented by a single particle, as schematically depicted on figure 2. The position of the probe particle is optimised according to classical force field combining van der Waals, electrostatic and Pauli forces acting between tip and sample. The PP-AM model provides good agreement with the experimental evidence as it can be seen from comparison of simulated AFM images shown on figure 3 with experimental counterparts presented on figure 4 for different tip-sample distances. This model provides not only a detailed understanding of the imaging mechanisms with functionalized tips but also represents a very efficient simulation tool (available online [41]).

These days, there are several more sophisticated theoretical approaches available for the high-resolution AFM modelling extending basics ideas of the PP model and employing inputs from total energy density functional theory (DFT) calculations [33, 42–44] too. It is worth to note that recently two papers [45, 46] reported sub-molecular contrast over molecules achieved with probes prepared with an intentional poking of metallic tip to surface, which may place of extra atom/molecule at the tip apex. Indeed, according to the PP–AFM model the faint sub-molecular contrast can be observed in tip-sample distances, where Pauli repulsion begins to compensate the attractive forces over areas of higher electron density (atoms/bonds). Nevertheless the bending of the probe particle is still negligible in these distances, as shown on figure 3. Thus, in principle, it is matter of spatial variation of interaction strength over inspected molecule and the signal-to-noise ratio of the frequency shift during data acquisition to achieve the sub-molecular resolution.

The precise origin of the STHM and IETS–STM imaging mechanism remained long under debate [16, 47]. Nevertheless Hapala *et al* showed that the mechanistic PP-model for high-resolution AFM images [39] can be successfully extended to both STM [39, 48] and the IETS–STM mode [33].

3. High-resolution AFM imaging

Figure 4 shows an evolution of simultaneously acquired AFM and STM images of PTCDA molecules on Ag(1 1 1) surface during the approach of a tip decorated with a single Xe atom [49, 50]. In the far tip-sample distance regime, the AFM contrast consists of a featureless oval rendering molecular contour. In intermediate tip-sample distances, the AFM contrast changes significantly clearly revealing characteristic benzene rings of PTCDA molecules. In very close distances, one can observe a characteristic bond sharpening, which is later accompanied with a contrast inversion. In particular, areas corresponding to the central part of benzene rings become more repulsive compared to those corresponding to molecular bonds and atoms. The contrast inversion effect is better visible in 3D plots of AFM images, shown in the left column of figure 4.

The characteristic evolution of the AFM contrast is driven by an interplay between different force components acting between functionalized tip and sample: attractive van der Waals (vdW), electrostatic and repulsive Pauli forces. What can be skipped is the chemical force reflecting a formation of the covalent/metal bond between outermost atoms of tip apex and sample [51, 52]. It is the presence of an inert molecule/atom at the tip apex, which reduces significantly chemical reactivity with respect to bare metallic tips. In principle, this substantially simplifies the theoretical description of tip-sample interaction avoiding demanding quantum mechanical calculations to capture the formation of chemical bonds.

The chemical inertness of the probe is an important prerequisite to achieve high-resolution contrast. It enables stable operation of the probe in the repulsive regime without undergoing irreversible changes. Noteworthily, the functionalized molecule/atom attached to the metallic tip base is mechanically the softest part of the whole tip-sample system. Consequently the mechanical stress induced by proximity of tip to surface is released mostly via a lateral relaxation of the probe particle and additional relaxation of the surface can typically be neglected. Of course, this assumption does not hold for complex non-planar molecules, which makes their

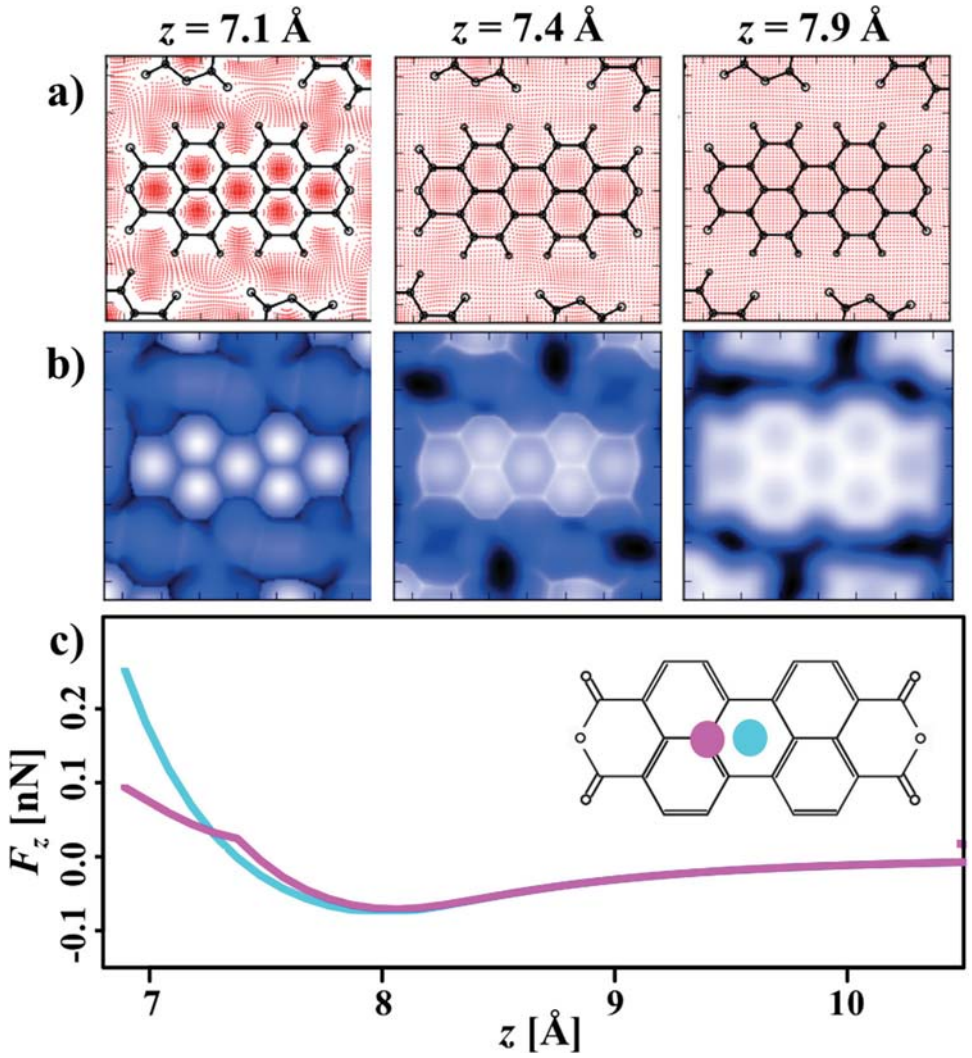

Figure 3. Calculated high-resolution AFM images of herringbone monolayer of PTCDA molecules deposited on Au(1 1 1) surface at different distances with the mechanistic PP-model: (a) lateral relaxation of the probe particle; (b) AFM (frequency shift) images and; (c) calculated vertical force F_z as a function of the tip-sample distance z measured over a carbon atom (pink) and the center of a benzene ring (turquoise; shown on inset of figure (c). Adapted with permission from [49], Copyrighted by the American Physical Society.

high-resolution imaging and its interpretation more difficult (as discussed later).

Let us discuss the role of each force component along the tip approach axis. In far tip-sample distances, vdW forces prevail giving rise to the blunt contrast over a molecule. On the other hand, in close tip-sample distances, it is the Pauli repulsion, which gives rise to the appearance of sharp edges in images. The sharp edges correspond to extremes (saddle points/ridges) of the potential energy surface, which the probe particle experiences in a given tip-sample distance [39, 40]. The saddle points of the potential energy surdaces are typically located over atoms or bonds where the Pauli repulsion fully compensates the attractive vdW and optionally electrostatic forces at a given tip-sample distance. At this distance, probe particle trajectories start to branch (bifurcate) to one or the other side of the saddle, as schematically depicted on figure 5(b). On the other hand, lateral position of the sharp edges is not sensitive to strength of Pauli repulsion even in close distances. This effect can be demonstrated employing a hard sphere model as described in supplemental materials of [50]. It is the electrostatic force, which can be both attractive and repulsive at different parts over an inspected molecule, responsible for variation of the lateral position of the intramolecular sharp edges [33, 50] as it will be discussed later.

In summary, we can say that the sharp features appearing in the AFM images always coincide with the borders of neighbouring basins of the potential energy surface. In other words, they coincide to the narrow areas, where the magnitude and direction of the lateral relaxation of the probe particle changes strongly upon small variations of the position of the tip relative to the sample (see figure 5). The large sensitivity of the lateral deflection of the probe particle on lateral position of tip near the saddle points causes the sharp image features in the AFM images, see figure 5(b).

3.1. Do the sharp lines always represent true bonds?

The position of the sharp lines in the high-resolution AFM images typically coincides with intramolecular bonds between atoms of a given molecule. Hence the appearance of the sharp

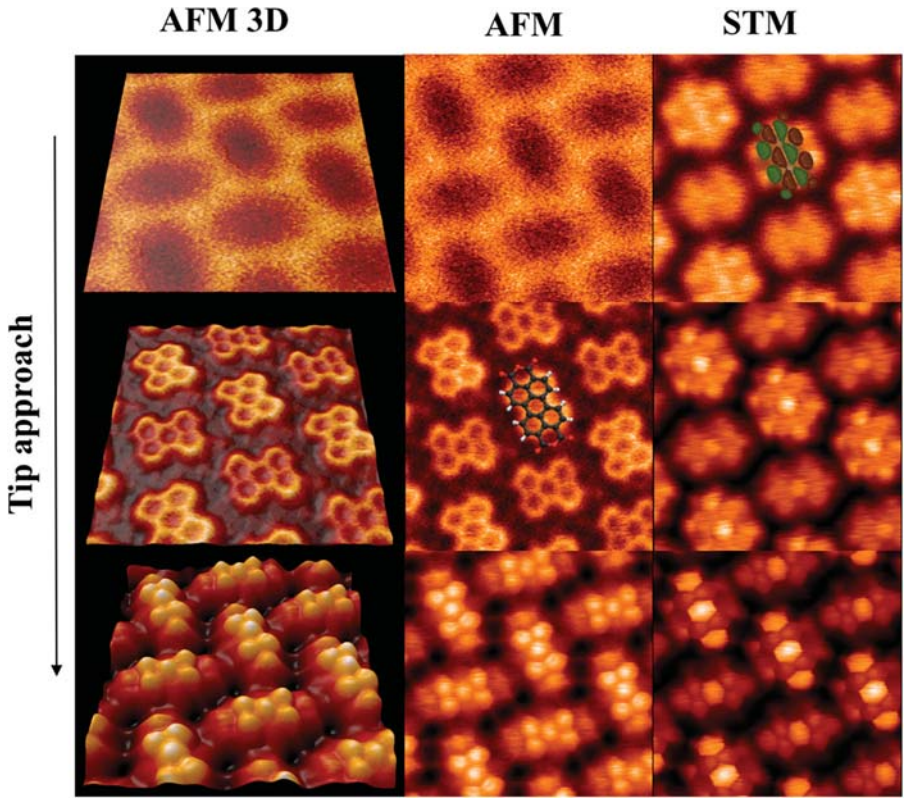

Figure 4. Evolution of high resolution AFM/STM contrast of PTCDA molecules on Ag(1 1 1) surface during approach of Xe-terminated tip: (Left column) series of constant height AFM images rendered in 3D for different tip sample distances. (Middle column) the same AFM images as these shown in the left column, but plotted in 2D perspective. Atomic structure of PTCDA molecule is superimposed over the AFM image. (Right column) series of constant height STM images acquired simultaneously with AFM channel [49]. Calculated LUMO orbital of PTCDA molecule is also displayed to show that it coincides well with the STM contrast observed in far distances.

lines tempts one to automatically interpret them as the true bonds [53]. However, Pavliček *et al* [54] found a pathological case, where the sharp edges can be also seen between two sulphur atoms, where there is no chemical bond established. This experimental evidence can be also reproduced by the PP-model, see figure 3 in [39]. On the other hand, Zhang *et al* [53] published high-quality AFM images of weakly bonded assemblies of guanine molecules on a metal surface, revealing clear sharp edges observed between the molecules. In addition, total energy density functional theory (DFT) calculations revealed enhanced accumulation of the electron density in locations where the sharp lines were experimentally observed. Based on this argument, they correlated these sharp lines to intermolecular hydrogen bonds formed between guanine molecules. Sweetman *et al* observed similar intermolecular sharp lines in high-resolution AFM images between naphthalene tetracarboxylic diimide molecules [55], matching expected positions of intermolecular hydrogen bonds. The fact that both experimental AFM contrasts [53, 55] can be reproduced well by the mechanistic PP-model [39] without taking explicitly into account distribution of the electron density opened a lively debate about the origin and the correct interpretation of these sharp intramolecular features.

To tackle this problem, Hamalainen *et al* [40] investigated a molecular system, where intermolecular bonds should or should not be present between neighbouring molecules. They found that sharp intermolecular features are detected in both regions. This finding clearly demonstrates that the intermolecular contrast cannot be automatically interpreted as true intermolecular bonds. These finding were also supported by theoretical modelling [40, 56]. Furthemore, very similar conclusions were also found in others works [57, 58].

Thus the possibility to conclusively identify the true intramolecular hydrogen bonds remains an open challenge. To clearly discriminate true bonds, one may think about simultaneous application of different techniques in a multi-pass mode. For example, one can employ first the high-resolution AFM/STM imaging to detect the position of sharp lines. Next, one can try to detect the presence of the IETS signal [59] characteristic for weak intermolecular hydrogen bonds in the marked intermolecular area. It has been shown recently that the IETS signal can be enhanced by a proper tip apex functionalization [60].

3.2. Impact of the electrostatic force on the AFM contrast

We already mentioned that the high-resolution AFM imaging mechanism is driven by the interplay between attractive van der Waals (vdW), electrostatic and repulsive Pauli forces acting between the functionalized tip and sample. Originally, only vdW and Pauli forces were considered in theoretical explanations [18, 34, 39, 40]. Therefore there is a question namely, what is the role of the electrostatic force in the imaging mechanism? The strength of the electrostatic force depends on the

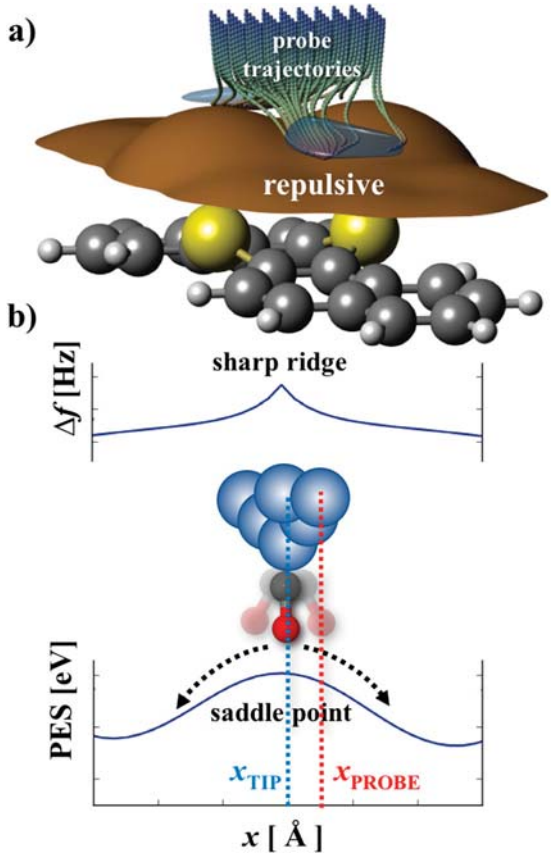

Figure 5. Explanation of the sharpening of AFM contrast as a consequence of lateral relaxation of probe particle in close distances: (a) Schematic view of the probe particle trajectory during tip approach represented by individual threads dominated by the Pauli repulsion energy. (b) Appearance of the sharp edge in the frequency shift Δf signal due to convex shape of the potential surface energy (PES) landscape causing probe particle relaxation at close distances. Adapted with permission from [39], Copyrighted by the American Physical Society.

charge density distribution (polarity) on probe and surface. Indeed, for non polar organic molecules, fairly good agreement between experimental and simulated AFM images can be achieved without the inclusion of the electrostatic force [39]. However, detailed analysis of different cases revealed that agreement with experimental evidence can be substantially improved, when the electrostatic force is included in the PP-model [33, 49]. What is more, the AFM contrast of polar molecules with strong internal charge redistribution can significantly change [61], even when scanning with different functionalized tips [50, 62], as shown on figure 6. This effect is caused by a displacement of the probe particle by the electrostatic field of the probed molecules during scanning. In other words, the movement of the probe particle induces the distortions of the positions of atoms and bonds seen in the high-resolution images, as shown on figure 7. This effect allows for mapping of the electrostatic field in the vicinity of the investigated molecules [50].

As another example, Van der Lit and coworkers [62] investigated AFM images of an ordered monolayer of bis-(para-benzoic acid) acetylene molecules acquired with different tip terminations: Xe and CO. They found that the brightness and contours of the AFM contrast are significantly affected by the tip termination. Using the PP-model including the electrostatic interaction, they deduced that the charge of the tip and its electrostatic interaction with the sample is crucial in determining the contrast and the tip relaxations. The impact of the electrostatic force on the AFM contrast was also discussed in details by Guo *et al* [43] for π-conjugated molecules and Ellner *et al* [42] for ionic surfaces.

In the PP-model, the electrostatic force is calculated from the Hartree surface potential obtained from fully relaxed total energy DFT calculations of a molecule on surface and an effective charge density on the probe particle [33], see also the schemtic depicted on figure 8. The effective PP charge density can be approximated by different multipoles [42, 50] including monopole, dipole or quadrupole. Moreover, the charge density distribution can be significantly affected by charge transfer between the atom/molecule on the apex and the metallic tip base. Thus it is important to understand and to correctly determine the charge distribution of functionalized tips. Comparisons between various instances of experimental evidence and modelling revealed [50, 62, 63] that a CO-terminated tip has only a very weak charge, while a Xe-terminated tip is positively polarised.

Ellner *et al* [42] showed that the overall picture can be more complex. They found that the electrostatic field of the CO-terminated metallic tip can be described as a superposition of two fields steaming from the metal base tip and the CO molecule. The interplay of these two fields with an opposite sign is fundamental to capture the contrast evolution of a Cl vacancy in bilayer NaCl on Cu(1 1 1) along the tip approach axis. While a dipole with its positive pole at the metallic tip dominates at far distance, a dipole located on the CO molecule, ith its negative end sticking out, prevails in close distances. Very recently, an analysis of a chiral AFM contrast obtained at far distance over a strongly polar water tetramer deposited on NaCl thin film with a CO-terminated tip can be well explained by a slightly negative (i.e. with its negative lobe pointing out towards the surface) quadrupole charge model for the probe particle [64]. It is evident that the charge distribution on different functionalized tips is still not completely understood and calls for more experimental and theoretical investigations.

It is also desirable to define new atomic or molecular candidates for tip functionalization [65, 66]. The main factors causing the wide usage of CO or Xe functionalized tips are (i) a well-defined and reproducible recipe for their preparation [21, 67–69], (ii) flexibility and stability of the molecule/atom on a metallic tip apex. However, the charge of such tips cannot be controlled easily. Better sensitivity could be achieved with functionalized tips having either large inherent charge or better polarizability. Ideal candidates would be small molecules or functional groups which could be easily charged by applied voltage. Therefore, we need to select new functionalization groups with tuneable charge/dipole/quadrupoles, easy polarisability and/or small redox potentials. Possible candidates are: hydroxyl groups, nitrile, isonitrile, nitrogen oxides, azide, quinones or transition metal chelates. For example, recent studies of ferrocene molecules have postulated them as an interesting candidate [70]. We also need to better understand

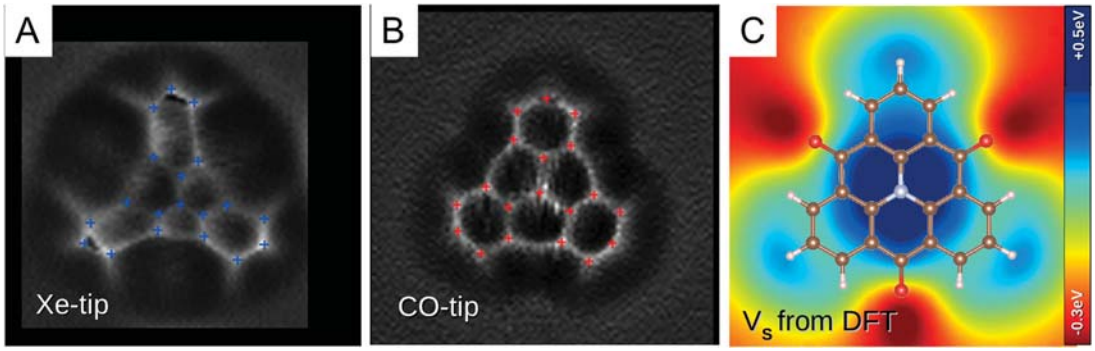

Figure 6. Variation of the high-resolution AFM contrast of TOAT molecule acquired with different probes. (a) Constant height high-resolution AFM image acquired with Xe-tip; (b) Constant height high-resolution AFM image acquired with CO-tip; (c) Calculated Hartree potential above TOAT molecule obtained from DFT simulations. Reproduced from [50]. CC BY 4.0.

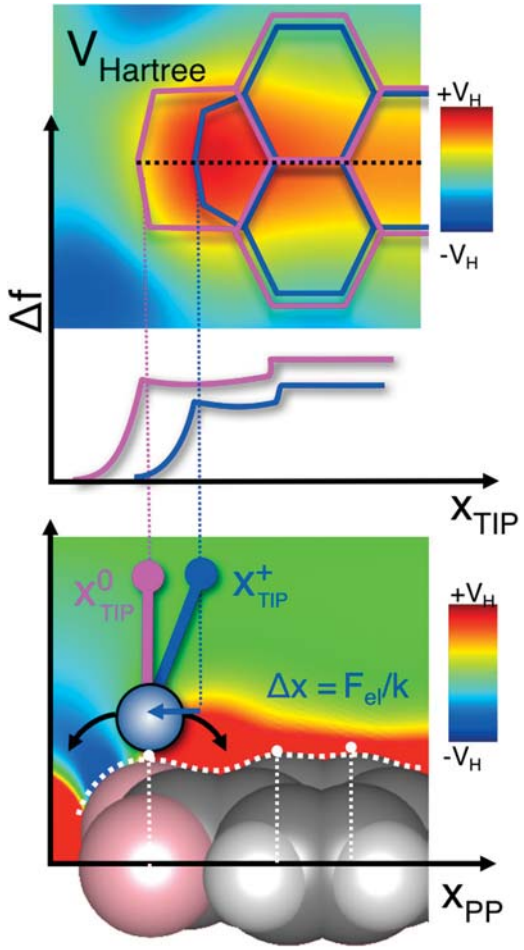

Figure 7. Schematic picture demonstrating the effect of lateral bending of the probe particle on the position of the sharp edges in high-resolution. (Upper) Blue and pink lines represent different positions of the sharp edges observed in high-resolution images acquired with the probe particles experiencing different lateral force. The position of the sharp edges in Δ f signal (AFM channel) changes accordingly. (Lower) Sideview of the lateral position of the probe particle x_{PP} with respect to the tip apex x_{TIP} experiencing a different lateral force at a saddle point. Background image renders calculated Hartree potential of a scanned (PTCDA) molecule, which induces the lateral bending Δx of the charged probe particle. Reproduced from [50]. CC BY 4.0.

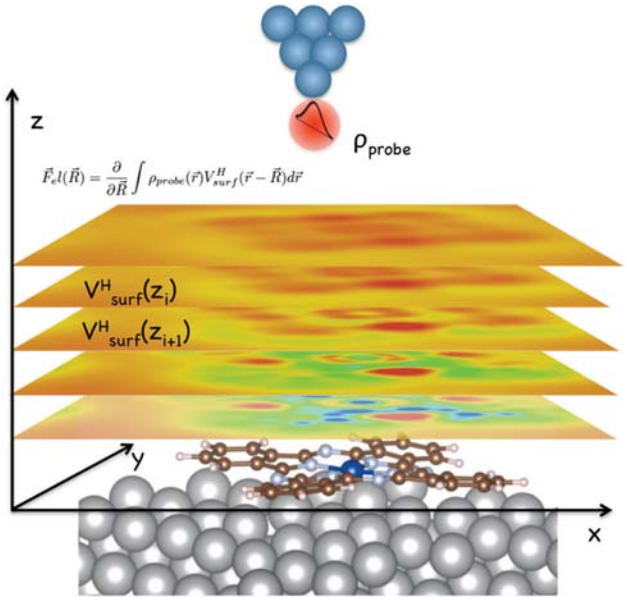

Figure 8. Schematic view of the electrostatic interaction acting between an effective charge on probe and Hartree potential on surface: The electrostatic interaction is calculated as derivative of convolution of the Hartree potential spanned on a rectangular grid obtained form total energy DFT calculations and an effective charge of the probe particle (red ball), for more details see [33].

how functionalized tips respond to changing bias voltage. As this we will be able to better evaluate their polarizability and possible charging. At the same time, we should search for the reliable and reproducible procedures for proper placement of the functional groups on the tip apex.

3.3. Going beyond low temperature limit

The sub-molecular resolution of individual molecules brought entirely new possibilities in the study of physical and chemical properties of individual molecules or their assemblies on surfaces. So far, it has been possible to carry out these measurements only at very low temperatures close to absolute zero with specially modified probes. As we discussed above, the modification consists of controlled positioning of just a

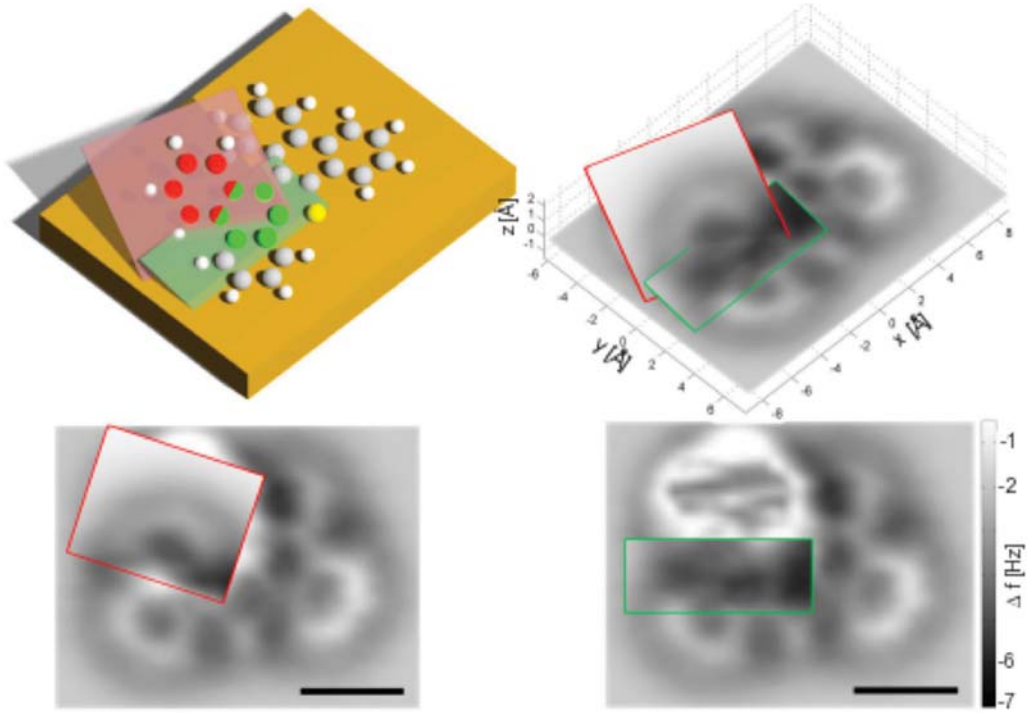

Figure 9. Reconstruction of molecular structure from 3D AFM data set of a non planar molecule. The sub-molecular resolution of an inspected non-planar molecule can be obtained from adjusting an angle under which cut-plane is performed. The figure is adopted with permission from [80]. Copyright (2015) American Chemical Society.

single molecule (e.g. carbon monoxide) or a noble gas atom on the apex of the metal tip. However, such tips are typically stable only at the very low temperatures. This condition has dramatically limited the applications of this method in terms relevant to important chemical and biological processes. For example, the possibility of imaging individual molecules on surfaces at ambient temperature represents an essential prerequisite for the study of catalytic reactions on solid surfaces at elevated temperatures.

Recently, the situation has changed in this direction. Several groups succeeded to obtain the sub-molecular resolution at liquid nitrogen temperature [58, 71]. What is more, Iwata *et al* [72] achieved sub-molecular resolution even at room temperature. Optimised scanning parameters enabled a significant enhancement of the frequency shift signal. Also the fact that the inspected PTCDA molecules were strongly bound to underlying silicon substrate facilitated the high-resolution imaging. According to supporting total energy DFT calculations compared with experimental force spectroscopies, a hydroxyl terminated silicon tip was proposed to be responsible for the enhancement of the contrast. Also Huber *et al* achieved intramolecular contrast on organic molecules at room temperature [73]. This achievement significantly advances the limits of the molecular resolution by means of scanning probe microscopy.

3.4. Imaging non-planar nanostructures and molecules

Another remaining challenge for the high-resolution technique is the imaging of complex non-planar molecules and nanostructures [74]. Especially, its application toward exploring species with structural flexibility and a distinct 3D character remains an open challenge. Recently, Emmrich *et al* [75] demonstrated that high-resolution AFM techniques can resolve individual atoms within metallic clusters deposited on surfaces. Consequently, the precise determination of the underlying surface symmetry of the few atoms clusters and their binding positions to different surface sites can be precisely determined. This is a formidable task, which cannot be achieved in standard STM mode. Very recently, the capability of non-invasive imaging of weakly bonded water clusters and 2D networks by the high-resolution AFM technique has been demonstrated [64, 76]. This opens new possibilities to characterise atomic structure of weakly bonded nano assemblies on surfaces.

In the case of imaging non-planar molecules, several remarkable achievements were also accomplished recently. First, O. Custance and his colleagues adopted a smart technique, so called dual-pass mode [71], which allowed sub-molecular resolution on C_{60} molecules at 77 K. Another approach to tackle this problem is based on a clever acquisition and analysis of the 3D data set of the frequency shift versus distance. Here the closest tip-sample approach is modulated from point to point for each tip approach to avoid tip damage due to an excessive repulsive tip-sample interaction. This is accomplished by retracting a tip when the frequency shift passes its minimum during approach and consequently its slope changes [77]. Using this approach, AFM can be employed as a powerful technique for the structural analysis of molecular adsorption position [78] or strongly non-planar molecules with a pronounced 3D character as demonstrated by Albrecht *et al* [79], see figure 9. In this way, the structure

of nonplanar molecules as well as their reaction products on different parts of surfaces (terraces and at step edges) can also be determined [80].

4. High-resolution STM imaging

We already discussed that a decoration of a metallic STM tip with the flexible atom/molecule leads to drastic changes of the observed STM contrast [12, 13, 15–17]. For example, STM images of PTCDA molecules deposited on Ag(1 1 1) surface acquired in close tip-sample distances, shown on figure 4 (right column), are significantly modified with respect to those in far tip-sample distances. Moreover, in comparing the character of the LUMO orbital (shown in inset of figure 4) with the STM contrast obtained in close distances, we can see that the STM picture has no resemblance to the typical LDOS images. Instead, it is more related to the chemical structure of PTCDA molecules. This trend holds for different functionalized tips [65].

In principle, the high-resolution STM imaging represents an experimentally less demanding way to achieve sub-molecular contrast than AFM or IETS–STM techniques. The STM mode posses several advantages with respect to the dynamical AFM mode [81]: (i) the tunnelling current generally behaves monotonically along the tip-sample distance; (ii) it has better signal to noise ratio than the AFM mode; (iii) instrumental STM setup is less complicated than with AFM; and (iv) STM operation is much simpler than dynamical AFM mode or IETS–STM. Furthermore, it provides information about both the electronic and atomic structure of the inspected molecules. Thus, information provided by STM is, in principle, superior to AFM method. On the other hand, while the origin of the high-resolution AFM was fairly well understood soon, the high-resolution STM mechanism remained longer under debate [16, 47]. I believe that it was mainly the lack of detailed understanding of the high-resolution STM imaging mechanism, which has impeded its wider application.

The STM contrast obtained with generic metallic tips is well understood in terms of the Bardeen approach [82] and its modification derived by Chen [83–85] or even the simpler Tersoff and Hamann approximation [86]. Different simulation schemes were devised based on non-perturbative [87–89] and perturbative approaches [90, 91]. The perturbative approach is only valid in far tip-sample distances, when the contact between tip and sample is not well developed [92]. Nevertheless, all these methods assume a rigid probe without taking into account any structural tip relaxation due to tip-sample interaction. However the relaxation of the functionalized tip is crucial for the understanding of the high-resolution contrast, as we already discussed above.

Already in the original version introducing the PP–AFM model [39], a simple STM model was proposed. It describes the conductance through the STM junction via two terms: (i) the tunnelling from a metallic tip base to the probe particle T_T; and (ii) subsequent tunneling from the probe particle to the sample T_i. The tunnelling rates were described via exponential hoppings, where values change according to the relaxation of the PP during tip approach as discussed in [39]. Surprisingly, this very simple STM model can reasonably reproduce sharp edges frequently observed in STM images, as it was demonstrated in the case of PTCDA/Ag(1 1 1) [39]. This indicates that the relaxation of the flexible PP attached to metallic tip is most likely responsible for the peculiar sub-molecular STM contrast.

However, the simple STM model [39] contains one severe simplification, which prevents general application of the model to an arbitrary molecular system. It neglects completely the electronic structure in the description of the tunneling process between tip and sample. Indeed, numerous experimental evidence [12, 15–17] indicates that the STM contrast depends on experimental conditions—such as applied bias voltage or the atomic and electronic structure of STM probe and substrate. Thus, it is not surprising that inclusion of the electronic structure of both tip and sample is mandatory to understand in detail the high-resolution STM imaging with functionalized tips.

Very recently Krejčí *et al* [48] introduced a more sophisticated but still computationally efficient STM model, which combines the mechanistic PP–AFM [39] and Chen's model for the tunneling process across a STM junction. The PP–AFM model introduces the PP relaxation, while the Chen's model deals with the electronic wave functions of tip and sample. The validity of the new STM model is supported by very good agreement with selected experimental STM images discussed in the original paper [48]. It was shown that the new PP–STM model is able to explain experimentally observed features, which could not be properly reproduced with either the original simple model [39] or traditional STM methods. The model demonstrates that the high-resolution STM mechanism consists of standard STM imaging, including electronic states of the sample and the tip apex orbital structure, but with the contrast heavily distorted by relaxation of the flexible functionalized tip apex.

To understand in details the influence of the mechanical PP relaxation and the electronic structure on the resulting STM contrast, one should analyze each of them separately. Figure 10(a) represents calculated STM images of a PTCDA molecule on Au(1 1 1) surface with a fixed CO-tip model. The STM contrast reveals a characteristic pattern, which transforms the original shape of the HOMO orbital into 5 stripes at each side of the molecule and 4 squares in the middle of it. This effect is the result of cancellation of the tunnelling current due to interference effects for a particular tip orbital symmetry [14]. The simulated STM contrast is very different from experimental evidence, which is shown on figure 10(d). The situation changes when we include the lateral relaxation of PP. Figure 10(b) represents fully optimised STM calculation, where the PP relaxation is included. The calculated STM image matches very well the experimental one. The impact of the PP relaxation can be better understood from the STM profile shown on figure 10(c). The lateral relaxation, which the PP undergoes above a central hexagon, locates the PP in the centre of the benzene ring. This has two fundamental consequences: (i) formation of the sharp edge, where the saddle point in the potential energy surface is located; and (ii)

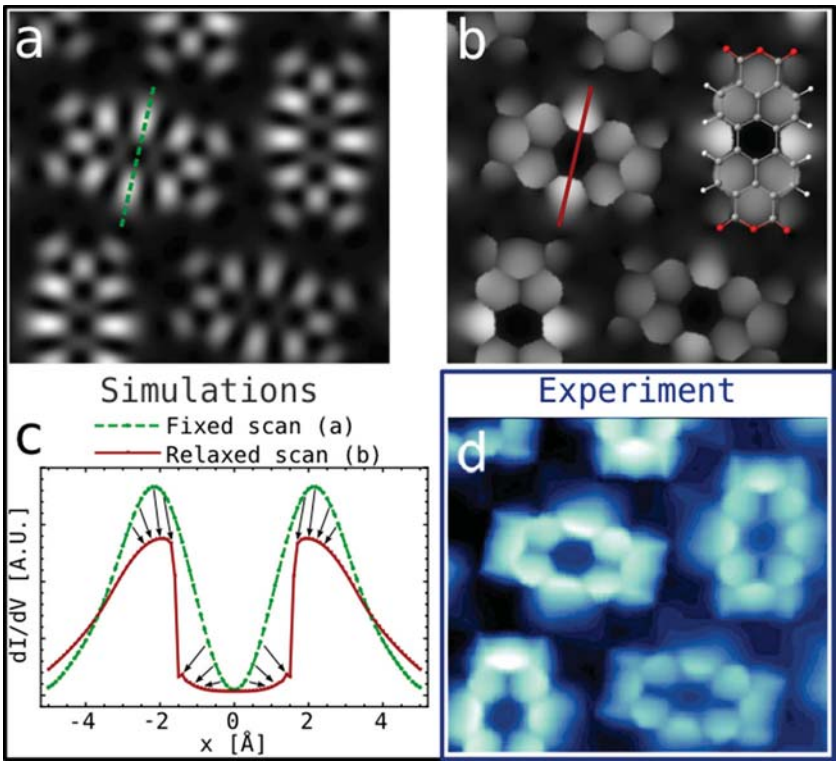

Figure 10. Effect of the lateral bending of the probe particle on the STM contrast and its comparison to experimental evidence: Calculated constant height dI/dV images of PTCDA/Au(1 1 1) at the energy of HOMO of PTCDA obtained with PP–STM code using p_x and p_y orbitals on the probe particle with the fixed (b) and relaxed (c) probe particle, respectively. (c) Profile lines taken above centers of PTCDA molecules as indicated in (b) and (c) by green dashed for fixed and red full line for relaxed probe particle, respectively. The arrows indicate the changes in the dI/dV signal given by the PP relaxations. (d) Experimental constant height HR-STM dI/dV figure of PTCDA/Au(1 1 1) obtained with CO tip at $V_{\text{bias}} = -1.6$ V [93]. For details see Krejčí *et al* [48].

the position of the PP remains almost unaltered while scanning over the central hexagon; consequently the STM signal remains almost constant. This gives rise to characteristic plateaus observed in the STM images.

From comparison between experimental and theoretical STM simulations we can also learn something about the electronic structure of functionalized tips. Krejčí *et al* [48] showed that STM images obtained with a Xe-tip can be reproduced very well with a s-like orbital on the PP. On the other hand, they found that STM images acquired with CO-tips are well mimicked with p_x and p_y orbitals on the PP. Gross *et al* [14] achieved good agreement for STM images obtained with CO tips in the far distance regime by taking into account linear combination of s, p_x and p_y orbitals on the probe. Pavlíček *et al* [94] claimed that the p and s contributions can depend on the applied bias voltage.

4.1. High-resolution IETS–STM imaging

The IETS–STM high-resolution technique introduced by Ho *et al* [32] maps out variations of the IETS signal corresponding to the frustrated translation (FT) mode of the CO-tip while scanning a molecule on the surface in close tip-sample distances. The variation of the IETS signal of FT mode at low bias set point (typically few meV) traces the chemical structure including characteristic sharp edges very similar to AFM and STM mode. This similarity with the other imaging modes points towards a joint mechanism behind them [33].

It is well known that a CO molecule placed on the tip or surface has two characteristic well-defined low energy excitation peaks corresponding to the frustrated translation and rotational mode [59]. It is only the frustrated translation mode, which exhibits distinct changes in the IETS signal when the CO-tip is approached towards the surface [95]. This is related to the low effective stiffness of the frustrated translational mode. which can be consequently modified by the tip-sample interaction. The energy of the frustrated translation vibrational mode of CO-tip was estimated to be ≈2.4 meV [32], which corresponds to an effective stiffness $k = 0.6\,\text{N m}^{-1}$; using $\epsilon = \hbar\sqrt{\frac{k}{m}}$, where m is the effective mass of the atom/molecule at the tip apex. This value matches very well with values presented by Gross *et al* [35]. They estimated the stiffness k of the CO-tip apex experimentally at $\approx 0.5\,\text{N m}^{-1}$ and total energy DFT calculations gave values within the range $0.3–1.6\,\text{N m}^{-1}$. Weymouth *et al* [37] obtained the stiffness $k = 0.24\,\text{N m}^{-1}$ by a thorough analysis of 3D frequency shift versus distance measurements of a CO-tip interacting with CO on the surface. The stiffness in the range of $0.25–0.6\,\text{N m}^{-1}$ was used in PP–AFM [39, 50, 62, 63] and PP–STM [48] simulations providing a good agreement with experimental evidence.

To explain the origin of the high-resolution IETS–STM mechanism, Hapala *et al* extended the PP–AFM model [39] including analysis of the vibrational modes of the PP [33]. Namely, they employed the standard dynamical matrix approach to evaluate the vibrational energy of the PP for a

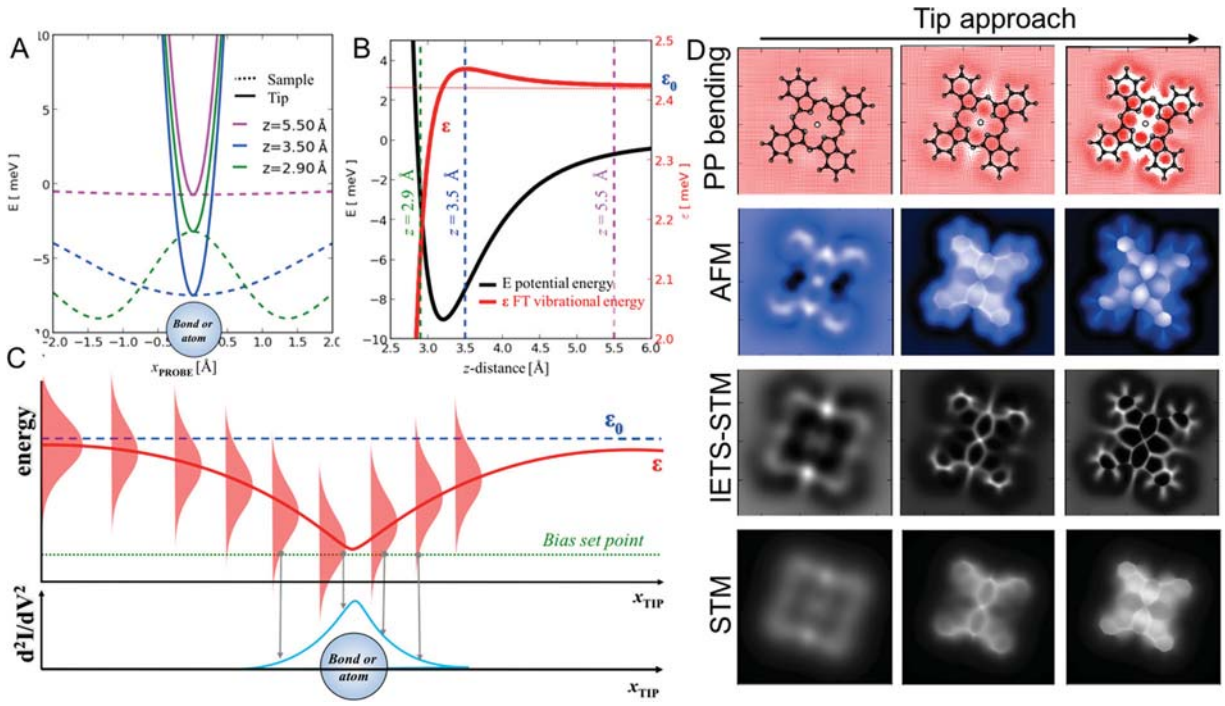

Figure 11. Explanation the origin of the IETS–STM contrast obtained with functionalized tips. (a) Interaction energies of the probe particle for different tip-sample distances consisting of V_{SPRING} (solid line) and varying V_{ATOM} (dashed line) for different positions above an atom on surface. (b) Variation of FT vibrational mode and the interaction energy with surface atom (V_{ATOM}) (black) with tip-sample distance. (c) Evolution of IETS–STM signal across a surface atom due to renormalisation of the energy of the FT vibrational mode (red). (d) correlation between the bending of the probe particle and the contrast in AFM, STM and IETS–STM images calculated for different tip-sample distances. Adapted with permission from [33], Copyrighted by the American Physical Society.

given tip position. In principle, the PP has three normal modes, where one mode is associated with the radial motion of the PP around the tip apex and two modes reflecting its lateral bending. The first radial mode is relatively stiff and it is not relevant for the analysis of the IETS signal. Nevertheless, the two other modes are much softer and they can be directly associated to the frustrated translation mode of a CO-tip. In the IETS–STM model, the vibrational energy of the lateral PP modes is set to be ≈2 meV for a free standing PP, which corresponds to the lateral PP stiffness $k = 0.6\,\mathrm{N\ m^{-1}}$. However, the FT vibrational energy varies during scanning due to the tip-sample interaction. Namely, the attractive (convex) and repulsive (concave) character of the surface potential induces vibration mode hardening and softening, respectively, as shown in figures 11((a) and (b)).

The model [33] convincingly showed that the IETS mechanism is related to a variation of the frustrated translational mode of a CO molecule placed at the tip apex, which responds sensitively to the changes of a local curvature of the surface potential. To explain the imaging IETS–STM mechanism in more details, let us consider a simple example depicted on figure 11(c). In this scenario, the PP is scanned across a bond/atom at a certain height. When located far from the atom/bond the FT vibrational energy remains unaltered because of negligible interaction of the PP with the substrate. However, when the PP is located above the bond/atom, its FT energy is consequently reduced by experiencing the repulsive interaction with the substrate. The IETS signal detected at a given bias set point is enhanced as shown in figure 11(c). Thus the modulation of FT modes of CO on the tip [95] and the consequent variation of the IETS signal gives rise to the characteristic contrast observed in high-resolution IETS–STM images. Worth to note that recent studies of IETS signal of the FT and FR modes of CO on the tip [96–98] provided more information about the inelastic tunnelling processes, but also generated new theoretical challenges for deeper understanding the mechanism.

We should note that the model explains the contrast only using the variation of the FT vibrational energy, but completely omits the intensity of the IETS signal. However detailed inspection of the experimental data [32] reveals that the variation of the intensity also contributes to the high-resolution IETS–STM contrast. Nevertheless, understanding of this phenomenon would require more sophisticated but computationally very demanding theoretical approaches [99].

It is interesting to compare high-resolution images of all the techniques calculated with the PP model [33]. Figure 11(d) displays simultaneously calculated high-resolution AFM, STM and IETS–STM images together with lateral bending of the PP position at different tip-sample distances. This comparison demonstrates that the sharpening of sub-molecular contrast is closely related to the lateral bending of the CO-probe in the repulsive regime. It also puts the IETS–STM imagining mechanism on

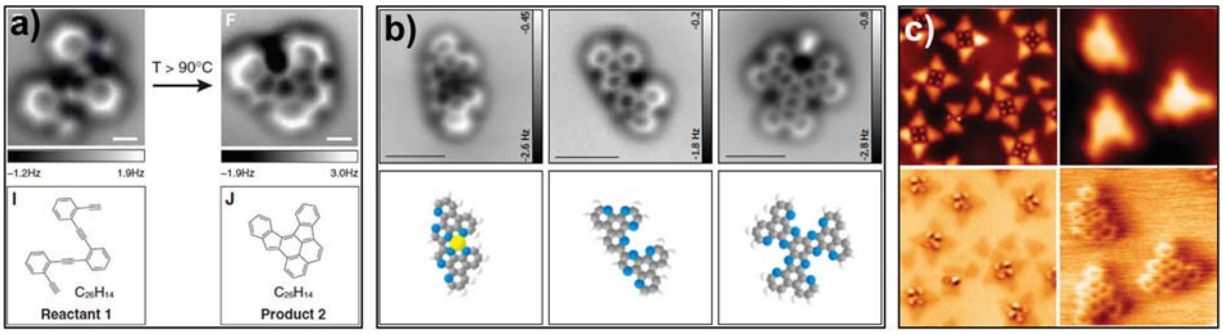

Figure 12. Examples of molecular products of on-surface reactions resolved with high-resolution AFM imaging. (a) cyclization of individual oligo-(phenylene-1,2-ethynylenes) molecules on Ag(1 0 0) surface From [27]. Reprinted with permission from AAAS. (b) Selected structures including organometallic complex formed after thermal annealing of pyrazino[2,3-f][4,7]phenanthroline on Au(1 1 1) surface. Reprinted with permission from [122]. Copyright (2016) American Chemical Society. (c) Chiral intermediates and final products of chemical transformation of dibenzo[i,o]heptahelicene on Ag(1 1 1) surface.

common ground with already established high-resolution AFM and STM mechanisms. The experimental evidence has been achieved very recently by de la Torre *et al* [100] by acquiring simultaneous high resolution AFM/STM/IETS imaging of iron(II) phthalocyanine (FePc) on Au(1 1 1) surface with CO-functionalized probe at 4 Kelvin.

5. Applications and perspectives

The development of high-resolution imaging has provided completely new perspectives for characterisation of molecular systems on surfaces with unprecedented spatial resolution [10]. But it has also promoted new kinds of studies, which have been impossible up to now. For example, the controlled decoration of metallic tips provides access to direct measurements of the interaction energies between selected molecular systems, which are at the edge of the detection schemes of other techniques [29–31]. The possibility to image the internal chemical structure of individual molecules is *a dream come true* not only for organic chemists. Now reactants, intermediates and products of chemical reactions can be identified on the single molecule level with the unprecedented resolution [27], see figure 12(a). But not only that, we can also learn information about the chemical and physical properties of inspected molecules in real space including bond order analysis [35] and distribution of the electron densities [50, 101].

5.1. Chemical analysis of single molecules

There are plenty of analytical methods, such as nuclear magnetic resonance (NMR), mass and infrared spectrometry, chromatography, etc which can provide detailed information about structural and chemical properties of any known molecules. However, such methods work with an ensemble of molecules. It is only the scanning probe microscopy technique, which enables studies of basic properties of a single molecule, including electronic [102] and mechanical properties [103] or self-assembling processes [104]. Until recently, the poor spatial resolution of the molecular systems limited possibilities of the scanning probe techniques to investigate chemically relevant processes.

This changed dramatically as the spatial resolution was substantially enhanced with the birth of the high-resolution techniques. The potential of the technique was conclusively demonstrated by Gross *et al* in their seminal paper [23] resolving the chemical structure of unknown molecules where other analytical methods failed. They investigated a molecule, called cephalandole-A , isolated from the Taiwanese Orchid by means of the high-resolution AFM technique. The molecule can adopt several variants with the same molecular weight and functional groups. This hampers the precise identification of its chemical structure using mass spectrometry and NMR analysis. Nevertheless the high-resolution AFM images allowed unambiguous determination of the spatial localization of the functional group and therefore the proper atomic structure. This result demonstrated fully the potential, which the high-resolution technique offers for studies of complex biological and chemical structures and processes.

Another relevant chemical information, which can be extracted from the high-resolution imaging with functionalized tips is bond order analysis of carbon-carbon bonds [35]. In other words, a subtle variation of distances between neighbour carbon atoms of planar organic molecules can be determined, which allows mapping out the bond order of individual bonds within the molecule. It is worth noting that the presence of triple C–C bonds is typically reflected by bright spots detected in the middle of sharp edges connecting carbon atoms when probed with a CO-tip [27, 62].

Chemical recognition is a long-standing handicap of the scanning probe technique. Several concepts were proposed employing the IETS signal to obtain vibrational fingerprints of adsorbed molecules [59, 105] or the maximum of the chemical force to identify the chemical identity of single surface atoms [106–108]. The second technique is based on detecting the strength of the chemical bond established between outermost tip and surface atoms, which can reveal the identity of inspected surface atoms. However this approach cannot be adopted for the high-resolution imaging performed with chemically inert functionalized tips, where a chemical bond cannot be established between tip and sample. Thus one has to search for a different concept providing chemical sensitivity on the atomic and molecular level. Recently, van der Heijden *et al* [63] showed that similar organic molecules of slightly

different chemical composition can be distinguished by acquiring 3D frequency shift data with a CO terminated tip, combined with theoretical analysis using the PP–AFM model. Namely, they use variation of the minimum value of the frequency shift signal and its corresponding tip-sample distance as a fingerprint responsible for the different chemical contrast. Thus different chemical composition of molecules can be discriminated. However a robust and transferable method, which provides chemical sensitivity to single atoms within a molecule is still missing.

One possibility to tackle this problem may lie in a combination of the AFM with other modes (STM,IETS and KPFM) supplemented with theoretical modelling. While the AFM mode can identify very well the chemical structure of molecules, i.e. molecular skeleton, it is not very sensitive to the chemical identity of individual atoms. On the other hand, the chemical composition will strongly modify the frontier orbitals, to which the STM mode is sensitive at a given bias voltage (using e.g. orbital imaging technique [13]). Afterwards one can carry out a series of quantum simulations of the given molecular skeleton but with different variants of chemical species until the STM contrast is matched [25]. Alternatively, the KPFM signal can also offer additional information to discriminate the chemical species within molecules.

5.2. Imaging charge distribution within molecules

The electrostatic field of molecules largely determines its behaviour, e.g. it affects preferred sites within the molecule, where chemical reactions with other compounds can take a place. It is also crucial to understand self-assembling processes of individual molecules forming e.g. supramolecules or determining the electron-hole pair dynamics in excited states. Thus the mapping of the electrostatic field in real space is an important task for scanning force microscopy, which is still not satisfactorily resolved. Kelvin probe force microscopy (KPFM) has been so far a widely used technique, which enables the mapping of the local contact potential difference (LCPD) [109] on atomic [110, 111] and molecular scale [112–114]. It was shown that the KPFM contrast can be substantially enhanced using functionalized probes [66, 112]. Nevertheless, the traditional KPFM method suffers from an unclear relation between the detected signal (LCPD) and the quantities of interest (charge distribution, electrostatic field). Furthermore, the proximity of the scanning probe near the surface induces undesired artifacts in KPFM measurements that give rise to spurious alteration of the measured signal [101]. Namely, reaching sub-molecular spatial resolution of KPFM signal is possible only in the very close distance regime, where the acquired signal is governed by the complex interplay of local electrostatic fields of tip and sample, their polarization, the bending of the probe and the presence of conductance through the tunnelling junction. This hinders precise determination of the charge distribution within a single molecule with the traditional KPFM technique.

Therefore there is strong demand to establish a new technique, which overcomes, at least partially, the drawbacks of the KPFM technique. Albrecht *et al* [101] introduced an alternative measuring protocol that allows removal of the aforementioned artifacts of KPFM. The method of detecting charge distribution, which is based on measuring the Kelvin probe force spectroscopy (KPFS) for two different voltages applied to the scanning probe. It allows mapping out the bond polarization between carbon and hydrogen atoms (C–H) and fluorine (C–F), respectively. On the other hand, theoretical interpretation of the contrast and the measured quantity is not well defined. Another method, so called scanning quantum dot microscopy (SQDM), follows variations of instabilities in Kelvin parabolas reflecting single electron charge states on a molecule attached on a metallic tip for certain applied bias voltages [115]. The SQDM method allows for the mapping of the electrostatic field only in far field regime: consequently its spatial resolution is moderate. Recently, Hapala and coworkers introduced a new method [50], which exploits deformations occurring in the high-resolution AFM/STM images due to the electrostatic interaction, as depicted schematically on figure 7. It has clear theoretical interpretation at the very close distance required to achieve sub-molecular resolution. Furthermore, the method enables simultaneous acquisition of the electrostatic field together with information about the chemical structure of the inspected molecule. On the other hand, it relies on the presence of the sharp edges, which limits its resolution outside of single molecules.

5.3. Tracking on-surface chemical reactions

Despite the advances of the on-surface chemistry to form molecular assemblies (see e.g. [116–119] , detailed understanding of elementary reaction steps including identification of intermediates and final chemical products has been a challenge for many years. This situation dramatically changed with the invention of high-resolution SPM imaging. In their seminal work, de Oteyza *et al* [27] demonstrated that individual reactants, intermediates and final products of thermally induced enediyne cyclization reactions can be identified with unprecedented resolution, see figure 12(a). This provides the unique insight into pathways of on-surface chemical reactions, which cannot be achieved by other techniques [120].

This breakthrough initiated large activities in studying chemical reactions on both metal and insulator surfaces. For example, the possibility to track down details of the process of chemical reactions in combination with theoretical simulations allowed new insight into the role of entropy and energy dissipated to substrate during chemical reactions [121]. It also allowed the study of the reversible generation of individual polycyclic aryne molecules [24], regioselectivity in formation of organometallic complexes [122] (see figure 12(b)), covalent fusion of tetrapyrroles to graphene edges [123] and understanding the chiral transfer in complex chemical transformation of helical molecules [28] (see figure 12(c)). Importantly, it has been shown by Schuler *et al* [124] that the presence of ultrathin NaCl films as the substrate enables stabilization of radicals (i.e. molecules with unpaired valence electrons).

The technique also became invaluable in characterization of growth processes of graphene nanoribbons [125–129] or other 2D materials [130], supramolecular structures [57, 114] or covalent networks [131]. The high-resolution imaging solved a critical industrial problem identifying different allotrophes of Asphaltenes [25, 74], which may have fundamental impact on oil production in the future. So it is not surprising that oil companies are interested in the high-resolution techniques nowadays. This activity can attract other potential industrial partners such as pharmaceutical or chemical companies. For more comprehensive information about applications in the field of chemical reactions on surfaces, I refer the reader to a very recent review written by Pavliček and Gross [11], where they summarise comprehensively the recent progress and perspectives of high-resolution imaging in the field of on-surface chemistry.

5.4. Exploring weak forces

The possibility to decorate tip with a molecule or noble gas atom may not only serve for obtaining high resolution, but can be used to study the interaction between selected functional groups of molecules or individual atoms. The force spectroscopy measurements [52] provide direct access to interaction energies between two outermost atoms/molecules located on surface and tip as a function of the distance between the studied objects. This kind of information is hardly accessible by other experimental techniques. Thus it opens completely new perspectives to study weakly interacting systems and to establish well-defined benchmarks for theoretical methods describing the weak interactions. This possibility was recognised very early by P. Liljeroth and colleagues [29], who performed force spectroscopy measurements between two CO molecules, placed on the surface and tip, respectively, as shown on figure 13. Several new studies including experimental and theoretical measurements have appeared recently [30, 31, 132].

The force spectroscopy technique can be easily extended into 3D force volume mapping [133–135], where the spectroscopy curves are measured systematically on a pre-defined grid on the surface. The 3D-mapping procedure is able to provide detailed spatial variation of the interaction force between tip and sample [136]. From this perspective, it can analyse not only the strength but also directionality of the bond established between tip and sample. It has been shown that 3D force spectroscopy with functionalized tips may provide the interaction potential between the molecule at the tip and the one at the sample [29, 37]. Combining the species-specific selectivity of the custom designed tips with the ability to quantify tip-sample interactions with site-specific accuracy opens new opportunities for the study of the non covalent bonding mechanism between two constituents in a very controlled way.

So far, this technique has been applied to previously established systems such as noble gases (Xe, Kr) or CO molecules. With a bit of ambition, one can think about direct measurement of interactions of different kinds of non covalent interactions, such as hydrogen, π or halogen bonds. For example halogen, chalcogen, and pnictogen bonds are now subject to

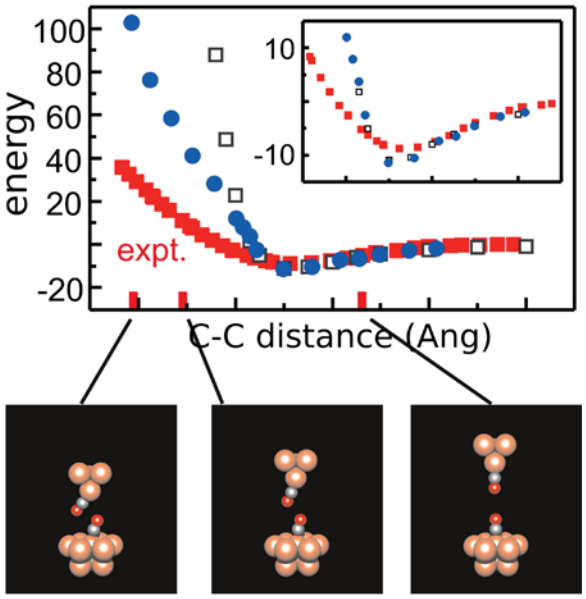

Figure 13. Measured interaction energy between two CO placed on surface and tip apex, respectively. The interaction energy acquired measured by AFM with gradual approach of CO-tip towards CO molecule on surface and corresponding theoretical calculations of CO–CO molecular junction. Reprinted with permission from [29], Copyright (2011) by the American Physical Society.

intensive research in chemistry. However, our understanding relies mostly on sophisticated but computationally demanding quantum chemistry methods. The possibility to directly measure interaction energy of selected functional groups with the σ-hole of a halogen atom, or even better to directly image the σ-hole by a functionalized tip, represents an invaluable source of information, and also establishing solid benchmarks for the high-level theories.

The hydrogen bond is another class of non-covalent bond, which again becomes the center of recent interest to scientists for its importance in biological systems. After nearly 100 years of existence of the concept, the hydrogen bonds got a new definition [137], which reflects these new developments and insights. From this perspective, the possibility to directly measure not only its strength but also directionality of non covalent bonds could bring more valuable information about their behaviour.

The main obstacle in the cases discussed above is not the measurements themselves, but rather a more suitable design of functional groups/molecules. We need not only molecules which remain stable upon deposition in UHV environment, but that can also adopt the most favourable mutual orientation when placed on tip and surface. Apparently, this task requires a close cooperation with gifted chemists.

6. Conclusions

The invention of high-resolution imaging techniques has initiated novel research lines and substantially advanced our possibilities to characterise molecules and nanostructures on surfaces under UHV conditions with unprecedented spatial resolution. The detailed understanding of the underlying

imaging mechanisms has allowed their exploitation providing new possibilities not only for imaging chemical structure of single molecules on surfaces but also to obtain valuable information about their chemical and physical properties. Furthermore, the underlying mechanism can be adopted to explain enhanced contrast observed in other scanning probe modes such as contact STM, liquid nc-AFM or electrochemical STM. These days, the high-resolution AFM/STM/IETS–STM techniques are well established and adopted by many research groups around the world. Many groups have mastered these techniques providing many exciting results in different fields. Several challenges remain open, such as spin resolution, chemical sensitivity, imaging complex non planar molecules etc. Nevertheless, these techniques have boosted new research lines, which were unimaginable before their development in just the last decade. In just this short period, it has become not only an indispensable tool in solving critical problems of fundamental science, but has also found industrial applications. Therefore I believe we can expect many new discoveries and surprises, as yet unforeseen today.

Acknowledgment

First I would like to specially thank to Prokop Hapala for his fundamental contribution to the formulation and development of the PP model, for deep-insight discussions and critical comments, Martin Švec for his key role in experimental activities in our laboratory and fruitful discussions and M. Ondráček, for valuable comments and critical revision of the manuscript. I would also like to thank to other colleagues from the Institute of Physics of CAS: O Krejčí, O Stetsovych, B de la Torre, Z Majzik, M Moro, P Mutombo, J Berger, M Telychko and A Cahlík. Special thanks to J Hellerstedt for his critical review of the manuscript. I'm indebted to following colleagues for inspired discussions and critical comments J Repp, F Albrecht, R Temirov, F J Tautz, J van der Lit, N J van der Heijden, I Swart, A Yakutovich, C Pignedoli, N Pavliček, L Gross, N Moll, G Meyer, P Pou, M Ternes, Y Sugimoto, P Liljeroth, F Schulz, F J Giessibl, K J Franke, I J Pascual, A Garcia-Lekue, T Fredericksen, A Arnau and P Hobza. Special thanks to J Repp, P Liljeroth, W Ho, L Gross, and M Crommie for their permission to publish selected Figures and providing their sources. I acknowledge the support by GAČR, grant no. 14-374527G, the Ministry of Education of the Czech Republic grants no. LM1015087 and 8E15B010, and Czech Academy of Sciences through Praemium Academiae award.

References

[1] Binnig G, Rohrer H, Gerber C and Weibel E 1982 Surface studies by scanning tunneling microscopy *Phys. Rev. Lett.* **49** 57–61
[2] Binnig G and Quate C F 1986 Atomic force microscope *Phys. Rev. Lett.* **56** 930–3
[3] Gewirth A and Niece B K 1997 Electrochemical applications of *in situ* scanning probe microscopy *Chem. Rev.* **97** 1129–62
[4] Stroscio J A and Celotta R J 2004 Controlling the dynamics of a single atom in lateral atom manipulation *Science* **306** 242–7
[5] Zhang Y-H, Wahl P and Kern K 2011 Quantum point contact microscopy *Nano Lett.* **11** 3838–43
[6] Schull G, Dappe Y J, González C, Bulou H and Berndt R 2011 Charge injection through single and double carbon bonds *Nano Lett.* **11** 3142–6
[7] Ido S, Kimiya H, Kobayashi K, Kominami H, Matsushige K and Yamada H 2014 Immunoactive two-dimensional self-assembly of monoclonal antibodies in aqueous solution revealed by atomic force microscopy *Nat. Mater.* **13** 264–70
[8] Fukuma T, Kobayashi K, Matsushige K and Yamada H 2005 True atomic resolution in liquid by frequency-modulation atomic force microscopy *Appl. Phys. Lett.* **87** 034101
[9] Jarvis S 2015 Resolving intra- and inter-molecular structure with non-contact atomic force microscopy *Int. J. Mol. Sci.* **16** 19936–59
[10] Gross L 2011 Recent advances in submolecular resolution with scanning probe microscopy *Nat. Chem.* **3** 273–8
[11] Pavliček N and Gross L 2017 Generation, manipulation and characterization of molecules by atomic force microscopy *Nat. Rev. Chem.* **1** 1–11
[12] Wagner C and Temirov R 2015 Tunnelling junctions with additional degrees of freedom: an extended toolbox of scanning probe microscopy *Prog. Surf. Sci.* **90** 194–222
[13] Repp J, Meyer G, Stojković S, Gourdon A and Joachim C 2005 Molecules on insulating films: scanning-tunneling microscopy imaging of individual molecular orbitals *Phys. Rev. Lett.* **94** 026803
[14] Gross L, Moll N, Mohn F, Curioni A, Meyer G, Hanke F and Persson M 2011 High-resolution molecular orbital imaging using a p-wave STM tip *Phys. Rev. Lett.* **107** 086101
[15] Temirov R, Soubatch S, Neucheva O, Lassise A C and Tautz F S 2008 A novel method achieving ultra-high geometrical resolution in scanning tunnelling microscopy *New J. Phys.* **10** 053012
[16] Weiss C, Wagner C, Kleimann C, Rohlfing M, Tautz S F and Temirov R 2010 Imaging Pauli repulsion in scanning tunneling microscopy *Phys. Rev. Lett.* **105** 086103
[17] Weiss C, Wagner C, Temirov R and Tautz F S 2010 Direct imaging of intermolecular bonds in scanning tunneling microscopy *J. Am. Chem. Soc.* **132** 11864–5
[18] Gross L, Mohn F, Moll N, Liljeroth P and Meyer G 2009 The chemical structure of a molecule resolved by atomic force microscopy *Science* **325** 1110–4
[19] Morita S, Wiesendanger R and Meyer E (ed) 2002 *Noncontact Atomic Force Microscopy* vol 1 (Berlin: Springer)
[20] Morita S, Giessibl F J and Wiesendanger R (ed) 2009 *Noncontact Atomic Force Microscopy* vol 2 (Berlin: Springer)
[21] Bartels L, Meyer G, Rieder K-H, Velic D, Knoesel E, Hotzel A, Wolf M and Ertl G 1998 Dynamics of electron-induced manipulation of individual CO molecules on Cu(1 1 1) *Phys. Rev. Lett.* **80** 2004–02007
[22] Morita S, Giessibl F J, Meyer E and Wiesendanger R (ed) 2015 *Noncontact Atomic Force Microscopy* vol 3 (Berlin: Springer)
[23] Gross L, Moll N, Meyer G, Ebel R, Abdel-Mageed W M and Jaspars M 2010 Organic structure determination using atomic-resolution scanning probe microscopy *Nat. Chem.* **2** 821–5
[24] Pavliček N, Schuler B, Collazos S, Moll N, Perez D, Guitin E, Meyer G, Pena D and Gross L 2015 On-surface generation and imaging of arynes by atomic force microscopy *Nat. Chem.* **7** 623–8
[25] Schuler B, Meyer G, Pena D, Mullins O C and Gross L 2015 Unraveling the molecular structures of asphaltenes by atomic force microscopy *J. Am. Chem. Soc.* **137** 9870–6

[26] Wickenburg S *et al* 2016 Tuning charge and correlation effects for a single molecule on a graphene device *Nat. Commun.* **7** 13553

[27] de Oteyza D G *et al* 2013 Direct imaging of covalent bond structure in single-molecule chemical reactions *Science* **340** 1434–7

[28] Stetsovych O, Švec M, Vacek J, Vacek Chocholoušová J, Jančařík A, Rybáček J, Kosmider K, Stará I G, Jelínek P and Starý I 2017 From helical to planar chirality by on-surface chemistry *Nat. Chem.* **9** 213–8

[29] Sun Z, Boneschanscher M, Swart I, Vanmaekelbergh D and Liljeroth P 2011 Quantitative atomic force microscopy with carbon monoxide terminated tips *Phys. Rev. Lett.* **106** 046104

[30] Corso M, Ondracek M, Lotze C, Hapala P, Franke K J, Jelínek P and Pascual J I 2015 Charge redistribution and transport in molecular contacts *Phys. Rev. Lett.* **115** 136101

[31] Kawai S, Foster A S, Björkman T, Nowakowska S, Björk J, Canova F F, Gade L H, Jung T A and Meyer E 2016 Van der Waals interactions and the limits of isolated atom models at interfaces *Nat. Commun.* **7** 11559

[32] Chiang C, Xu C, Han Z and Ho W 2014 Real-space imaging of molecular structure and chemical bonding by single-molecule inelastic tunneling probe *Science* **344** 885–8

[33] Hapala P, Temirov R, Tautz F S and Jelínek P 2014 Origin of high-resolution IETS–STM images of organic molecules with functionalized tips *Phys. Rev. Lett.* **113** 226101

[34] Moll N, Gross L, Mohn F, Curioni A and Meyer G 2010 The mechanisms underlying the enhanced resolution of atomic force microscopy with functionalized tips *New J. Phys.* **12** 125020

[35] Gross L, Mohn F, Moll N, Schuler B, Criado A, Guitian E, Pena D, Gourdon A and Meyer G 2012 Bond-order discrimination by atomic force microscopy *Science* **337** 1326–9

[36] Welker J and Giessibl F J 2012 Revealing the angular symmetry of chemical bonds by atomic force microscopy *Science* **336** 444–9

[37] Weymouth A J, Hofmann T and Giessibl F J 2014 Quantifying molecular stiffness and interaction with lateral force microscopy *Science* **343** 1120–2

[38] Neu M, Moll N, Gross L, Meyer G, Giessibl F J and Repp J 2014 Image correction for atomic force microscopy images with functionalized tips *Phys. Rev.* B **89** 205407

[39] Hapala P, Kichin G, Wagner C, Tautz F S, Temirov R and Jelínek P 2014 Mechanism of high-resolution STM/AFM imaging with functionalized tips *Phys. Rev.* B **90** 085421

[40] Hämäläinen S K, van der Heijden N, van der Lit J, den Hartog S, Liljeroth P and Swart I 2014 Intermolecular contrast in atomic force microscopy images without intermolecular bonds *Phys. Rev. Lett.* **113** 186102

[41] 2015 The probe particle model is available online on http://nanosurf.fzu.cz/ppr/

[42] Ellner M, Pavliček N, Pou P, Schuler B, Moll N, Meyer G, Gross L and Perez March R 2016 The electric field of CO tips and its relevance for atomic force microscopy *Nano Lett.* **16** 1974–80

[43] Guo M A, Van Hove C-S, Ren X and Zhao Y 2015 High-resolution model for noncontact atomic force microscopy with a flexible molecule on the tip apex *J. Phys. Chem.* C **119** 1483–8

[44] Sakai Y, Lee A J and Chelikowsky J R 2016 First-principles atomic force microscopy image simulations with density embedding theory *Nano Lett.* **16** 3242–6

[45] Mönig H, Hermoso D R, Arado O D, Todorović M, Timmer A, Schüer S, Langewisch G, Perez R and Fuchs H 2016 Submolecular imaging by noncontact atomic force microscopy with an oxygen atom rigidly connected to a metallic probe *ACS Nano* **10** 1201–9

[46] Hauptmann N, Robles R, Abufager P, Lorente N and Berndt R 2016 AFM imaging of mercaptobenzoic acid on Au(1 1 0): submolecular contrast with metal tips *J. Phys. Chem. Lett.* **7** 1984

[47] Martínez J, Abad E, González C, Flores F and Ortega J 2012 Improvement of scanning tunneling microscopy resolution with H-sensitized tips *Phys. Rev. Lett.* **108** 246102

[48] Krejči O, Hapala P, Ondráček M and Jelínek P 2017 Mapping the electrostatic force field of single molecules from high-resolution scanning probe images *Phys. Rev.* B **95** 045407

[49] Hapala P, Ondráček M M, Stetsovych O, Švec M and Jelínek P 2015 *Simultaneous nc-AFM/STM Measurements with Atomic Resolution* (Berlin: Springer) ch 3, pp 29–49

[50] Hapala P, Švec M, Stetsovych O, van der Heijden N J, Ondracek M, van der Lit J, Mutombo P, Swart I and Jelínek P 2016 Mapping the electrostatic force field of single molecules from high-resolution scanning probe images *Nat. Commun.* **7** 11560

[51] Pérez R, Payne M C, Štich I and Terakura K 1997 Role of covalent tip-surface interactions in noncontact atomic force microscopy on reactive surfaces *Phys. Rev. Lett.* **78** 678–81

[52] Lantz M A, Hug H J, Hoffmann R, van Schendel P J A, Kappenberger P, Martin S, Baratoff A and Güntherodt March H-J 2001 Quantitative measurement of short-range chemical bonding forces *Science* **291** 2580–3

[53] Zhang J, Chen P, Yuan B, Ji W, Cheng Z and Qiu X 2013 Real-space identification of intermolecular bonding with atomic force microscopy *Science* **342** 611–4

[54] Pavliček N, Herranz-Lancho C, Fleury B, Neu M, Niedenführ J, Ruben M and Repp J 2013 High-resolution scanning tunneling and atomic force microscopy of stereochemically resolved dibenzo[a,h]thianthrene molecules *Phys. Status Solidi* B **250** 2424–30

[55] Sweetman A M, Jarvis S P, Sang H, Lekkas I, Rahe P, Wang Y, Wang J, Champness N R, Kantorovich L and Moriarty P 2014 Mapping the force field of a hydrogen-bonded assembly *Nat. Commun.* **5** 3931

[56] Guo C-S, Xin X, Van Hove M A, Ren X and Zhao Y 2015 Origin of the contrast interpreted as intermolecular and intramolecular bonds in atomic force microscopy images *J. Phys. Chem.* C **119** 14195–200

[57] Kawai S, Sadeghi A, Xu F, Peng L, Orita A, Otera J, Goedecker S and Meyer E 2015 Extended halogen bonding between fully fluorinated aromatic molecules *ACS Nano* **9** 2574–83

[58] Sweetman A, Jarvis S P, Rahe P, Champness N R, Kantorovich L and Moriarty P 2014 Intramolecular bonds resolved on a semiconductor surface *Phys. Rev.* B **90** 165425

[59] Stipe B C, Rezaei M A and Ho W 1998 Single-molecule vibrational spectroscopy and microscopy *Science* **280** 1732–5

[60] Guo J, Lu J T, Feng Y, Chen J, Peng J, Lin Z, Meng X, Wang Z, Li X Z, Wang E G and Jiang Y 2016 Nuclear quantum effects of hydrogen bonds probed by tip-enhanced inelastic electron tunneling *Science* **352** 321–5

[61] Moll N *et al* 2014 Image distortions of a partially fluorinated hydrocarbon molecule in atomic force microscopy with carbon monoxide terminated tips *Nano Lett.* **14** 6127–31

[62] van der Lit J, Di Cicco F, Hapala P, Jelínek P and Swart I 2016 Submolecular resolution imaging of molecules by atomic force microscopy: the influence of the electrostatic force *Phys. Rev. Lett.* **116** 096102–5

[63] van der Heijden N J, Hapala P, Rombouts J A, van der Lit J, Smith D, Mutombo P, Švec M, Jelínek P and Swart I 2016 Characteristic contrast in Δf_{min} maps of organic molecules using atomic force microscopy *ACS Nano* **10** 8517–25

[64] Peng J, Guo J, Hapala P, Cao D, Ondráček M, Cheng B, Xu L, Jelínek P, Wang E and Jiang Y 2017

Submolecular-resolution non-invasive imaging of interfacial water with atomic force microscopy (arXiv:1703.04400)
[65] Kichin G, Weiss C, Wagner C, Tautz F S and Temirov R 2011 Single molecule and single atom sensors for atomic resolution imaging of chemically complex surfaces *J. Am. Chem. Soc.* **133** 16847–51
[66] Mohn F, Schuler B, Gross L and Meyer G 2013 Different tips for high-resolution atomic force microscopy and scanning tunneling microscopy of single molecules *Appl. Phys. Lett.* **102** 073109
[67] Heinrich A J, Lutz C P, Gupta J A and Eigler D M 2002 Molecule cascades *Science* **298** 1381
[68] Eigler D M and Schweizer E K 1990 Positioning single atoms with a scanning tunnelling microscope *Nature* **344** 524
[69] Bartels L, Meyer G and Rieder K H 1997 Controlled vertical manipulation of single CO molecules with the scanning tunneling microscope: a route to chemical contrast *Appl. Phys. Lett.* **71** 213
[70] Ormaza M *et al* 2017 Efficient spin-flip excitation of a nickelocene molecule *Nano Lett.* **17** 1877
[71] Moreno C, Stetsovych O, Shimizu T K and Custance O 2015 Imaging three-dimensional surface objects with submolecular resolution by atomic force microscopy *Nano Lett.* **15** 2257–62
[72] Iwata K, Yamazaki S, Mutombo P, Hapala P, Ondráček M, Jelínek P and Sugimoto Y 2015 Chemical structure imaging of a single molecule by atomic force microscopy at room temperature *Nat. Commun.* **6** 7766
[73] Huber F, Matencio S, Weymouth A J, Ocal C, Barrena E and Giessibl F J 2015 Intramolecular force contrast and dynamic current-distance measurements at room temperature *Phys. Rev. Lett.* **115** 066101
[74] Schuler B *et al* 2017 Characterizing aliphatic moieties in hydrocarbons with atomic force microscopy *Chem. Sci.* **8** 2315–20
[75] Emmrich M *et al* 2015 Subatomic resolution force microscopy reveals internal structure and adsorption sites of small iron clusters *Science* **348** 308–11
[76] Shiotari A and Sugimoto Y 2017 Ultrahigh-resolution imaging of water networks by atomic force microscopy *Nat. Commun.* **8** 14313
[77] Schuler B, Liu W, Tkatchenko A, Moll N, Meyer G, Mistry A, Fox D and Gross L 2011 Measuring the short-range force field above a single molecule with atomic resolution *Appl. Phys. Lett.* **99** 053106
[78] Schuler B, Liu W, Tkatchenko A, Moll N, Meyer G, Mistry A, Fox D and Gross L 2013 Adsorption geometry determination of single molecules by atomic force microscopy *Phys. Rev. Lett.* **111** 106103
[79] Albrecht F, Bischoff F, Auwärter W, Barth J V and Repp J 2016 Direct identification and determination of conformational response in adsorbed individual nonplanar molecular species using noncontact atomic force microscopy *Nano Lett.* **16** 7703–9
[80] Albrecht F, Pavliček N, Coral H-L, Mario R and Repp J 2015 Characterization of a surface reaction by means of atomic force microscopy *J. Am. Chem. Soc.* **137** 7424–8
[81] Giessibl F J 2003 Advances in atomic force microscopy *Rev. Mod. Phys.* **75** 949–83
[82] Bardeen J 1961 Tunnelling from a many-particle point of view *Phys. Rev. Lett.* **6** 57–9
[83] Chen C J 1990 Tunneling matrix elements in three-dimensional space: the derivative rule and the sum rule *Phys. Rev.* B **42** 8841–57
[84] Chen C J 2008 *Introduction to Scanning Tunneling Microscopy* vol 2 (New York: Oxford University Press)
[85] Mándi G and Palotás K 2015 Chen's derivative rule revisited: role of tip-orbital interference in stm *Phys. Rev.* B **91** 165406
[86] Tersoff J and Hamann D R 1985 Theory of the scanning tunneling microscope *Phys. Rev.* B **31** 805–13
[87] Cerdá J, Van Hove M A, Sautet P and Salmeron M 1997 Efficient method for the simulation of STM images. I. Generalized green-function formalism *Phys. Rev.* B **56** 15885–99
[88] Mingo N, Jurczyszyn L, Garcia-Vidal F J, Saiz-Pardo R, de Andres P L, Flores F, Wu S Y and More W 1996 Theory of the scanning tunneling microscope: Xe on Ni and Al *Phy. Rev.* B **54** 2225–35
[89] Blanco J M, Flores F and Pérez R 2006 Stm-theory: image potential, chemistry and surface relaxation *Prog. Surf. Sci.* **81** 403–43
[90] Hofer W A 2003 Challenges and errors: interpreting high resolution images in scanning tunneling microscopy *Prog. Surf. Sci.* **71** 147–83 (*Proc. of the* {*IXth*} *Symp. on Surface Physics, Trest Castle 2002*)
[91] Palotás K, Mándi G and Szunyogh L 2012 Orbital-dependent electron tunneling within the atom superposition approach: theory and application to w(1 1 0) *Phys. Rev.* B **86** 235415
[92] Blanco J M, Gonzalez C, Jelínek P, Ortega J, Flores F and Perez R 2004 First-principles simulations of stm images: from tunneling to the contact regime *Phys. Rev.* B **70** 085405
[93] Kichin G, Wagner C, Tautz F S and Temirov R 2013 Calibrating atomic-scale force sensors installed at the tip apex of a scanning tunneling microscope *Phys. Rev.* B **87** 081408
[94] Pavliček N, Swart I, Niedenführ J, Meyer G and Repp J 2013 Symmetry dependence of vibration-assisted tunneling *Phys. Rev. Lett.* **110** 136101
[95] Vitali L, Ohmann R, Kern K, Garcia-Lekue A, Frederiksen T, Sánchez-Portal D and Arnau A 2010 Surveying molecular vibrations during the formation of MetalMolecule nanocontacts *Nano Lett.* **10** 657–60
[96] Xu C, Chiang C-L, Han Z and Ho W 2016 Nature of asymmetry in the vibrational line shape of single-molecule inelastic electron tunneling spectroscopy with the STM *Phys. Rev. Lett.* **116** 166101
[97] Okabayashi N, Gustafsson A, Peronio A, Paulsson M, Arai T and Giessibl F J 2016 Influence of atomic tip structure on the intensity of inelastic tunneling spectroscopy data analyzed by combined scanning tunneling spectroscopy, force microscopy, and density functional theory *Phys. Rev.* B **93** 165415–6
[98] Han Z, Czap G, Xu C, Chiang C-L, Yuan D, Wu R and Ho W 2017 Probing intermolecular coupled vibrations between two molecules *Phys. Rev. Lett.* **118** 036801
[99] Frederiksen T, Paulsson M, Brandbyge M and Jauho A-P 2007 Inelastic transport theory from first principles: methodology and application to nanoscale devices *Phys. Rev.* B **75** 205413
[100] de la Torre B, Švec M, Krejčí O, Zbořil R and Jelínek P (in preparation)
[101] Albrecht F, Repp J, Fleischmann M, Scheer M, Ondracek M and Jelínek P 2015 Probing charges on the atomic scale by means of atomic force microscopy *Phys. Rev. Lett.* **115** 076101
[102] Aradhya S V and Venkataraman L 2013 Single-molecule junctions beyond electronic transport *Nat. Nanotechnol.* **8** 399–410
[103] Rascón-Ramos H, Artés J M, Li Y and Hihath J 2015 Binding configurations and intramolecular strain in single-molecule devices *Nat. Mater.* **14** 517–22
[104] Barth J V, Costantini G and Kern K 2005 Engineering atomic and molecular nanostructures at surfaces *Nature* **437** 671–9

[105] Pascual J I, Lorente N, Song Z, Conrad H and Rust H P 2003 Selectivity in vibrationally mediated single-molecule chemistry *Nature* **423** 525–8

[106] Setvín M, Mutombo P, Ondracek M, Majzik Z, Švec M, Cháb V, Ošt'ádal I, Sobotík P and Jelínek P 2012 Chemical identification of single atoms in heterogeneous III–IV chains on Si(1 0 0) surface by means of nc-AFM and DFT calculations *ACS Nano* **6** 6969–76

[107] Sugimoto Y, Pou P, Abe M, Jelínek P, Perez R, Morita S and Custance O 2007 Chemical identification of individual surface atoms by atomic force microscopy *Nature* **446** 64–7

[108] Onoda J, Ondráček M, Jelínek P and Sugimoto Y 2017 Electronegativity determination of individual surface atoms by atomic force microscopy *Nat. Commun.* **8** 15155

[109] Sadewasser S and Glatzel T (ed) 2012 *Kelvin Probe Force Microscopy: Measuring and Compensating Electrostatic Forces* (Berlin: Springer)

[110] Gross L, Mohn F, Liljeroth P, Repp J, Giessibl F J and Meyer G 2009 Measuring the charge state of an adatom with noncontact atomic force microscopy *Science* **324** 1428–31

[111] Gross L, Schuler B, Mohn F, Moll N, Pavliček N, Steurer W, Scivetti I, Kotsis K, Persson M and Meyer G 2014 Investigating atomic contrast in atomic force microscopy and Kelvin probe force microscopy on ionic systems using functionalized tips *Phys. Rev.* B **90** 155455

[112] Mohn F, Gross L, Moll N and Meyer G 2012 Imaging the charge distribution within a single molecule *Nat. Nanotechnol.* **7** 227–31

[113] Schuler B, Liu S, Geng Y, Decurtins S, Meyer G and Gross L 2014 Contrast formation in Kelvin probe force microscopy of single π-conjugated molecules *Nano Lett.* **14** 3342–6

[114] Kawai S *et al* 2013 Obtaining detailed structural information about supramolecular systems on surfaces by combining high-resolution force microscopy with *ab initio* calculations *ACS Nano* **7** 9098–105

[115] Wagner C, Green M F B, Leinen P, Deilmann T, Krüger P, Rohlfing M, Temirov R and Tautz F S 2015 Scanning quantum dot microscopy *Phys. Rev. Lett.* **115** 026101

[116] Barth J V 2007 Molecular architectonic on metal surfaces *Ann. Rev. Phys. Chem.* **58** 375–407

[117] Grill L, Dyer M, Lafferentz L, Persson M, Peters M V and Hecht S 2007 Nano-architectures by covalent assembly of molecular building blocks *Nat. Nanotechnol.* **2** 687–91

[118] Swart I, Gross L and Liljeroth P 2011 Single-molecule chemistry and physics explored by low-temperature scanning probe microscopy *Chem. Commun.* **47** 9011

[119] Klappenberger F, Zhang Y-Q, Björk J, Klyatskaya S, Ruben M and Barth J V 2015 On-surface synthesis of carbon-based scaffolds and nanomaterials using terminal alkynes *Acc. Chem. Res.* **48** 2140–50

[120] Riss A *et al* 2014 Local electronic and chemical structure of oligo-acetylene derivatives formed through radical cyclizations at a surface *Nano Lett.* **14** 2251–5

[121] Riss A *et al* 2016 Imaging single-molecule reaction intermediates stabilized by surface dissipation and entropy *Nat. Chem.* **8** 678–83

[122] Kocić N, Liu X, Chen S, Decurtins S, Krejčí O, Jelínek P, Repp J and Liu S-X 2016 Control of reactivity and regioselectivity for on-surface dehydrogenative aryl–Aryl bond formation *J. Am. Chem. Soc.* **138** 5585–93

[123] He Y, Garnica M, Bischoff F, Ducke J, Bocquet M-L, Batzill M, Auwarter W and Barth J V 2016 Fusing tetrapyrroles to graphene edges by surface-assisted covalent coupling *Nat. Chem.* **9** 33–8

[124] Schuler B, Fatayer S, Mohn F, Moll N, Pavliček N, Meyer G, Pena D and Gross L 2016 Reversible Bergman cyclization by atomic manipulation *Nat. Chem.* **8** 220–4

[125] Ruffieux P *et al* 2016 On-surface synthesis of graphene nanoribbons with zigzag edge topology *Nature* **531** 489–92

[126] Dienel T, Kawai S, Söde H, Feng X, Müllen K, Ruffieux P, Fasel R and Gröning O 2015 Resolving atomic connectivity in graphene nanostructure junctions *Nano Lett.* **15** 5185–90

[127] Kawai S, Saito S, Osumi S, Yamaguchi S, Foster A S, Spijker P and Meyer E 2015 Atomically controlled substitutional boron-doping of graphene nanoribbons *Nat. Commun.* **6** 8098

[128] Talirz L, Ruffieux P and Fasel R 2016 On-surface synthesis of atomically precise graphene nanoribbons *Adv. Mater.* **28** 6222–31

[129] Schulz F *et al* 2017 Precursor geometry determines the growth mechanism in graphene nanoribbons *J. Phys. Chem.* C **121** 2896–904

[130] Barja S *et al* 2016 Observation of charge density wave order in 1D mirror twin boundaries of single-layer MoSe2 *Nat. Phys.* **12** 751–6

[131] Kawai S *et al* 2016 Thermal control of sequential on-surface transformation of a hydrocarbon molecule on a copper surface *Nat. Commun.* **7** 12711–7

[132] Wagner C, Fournier N, Ruiz V G, Li C, Mullen K, Rohlfing M, Tkatchenko A, Temirov R and Tautz F S 2014 Non-additivity of molecule-surface van der Waals potentials from force measurements *Nat. Commun.* **5** 5568

[133] Hölscher H, Langkat S M, Schwarz A and Wiesendanger R 2002 Measurement of three-dimensional force fields with atomic resolution using dynamic force spectroscopy *Appl. Phys. Lett.* **81** 4428–30

[134] Ternes M, Lutz C P, Hirjibehedin C F, Giessibl F J and Heinrich A J 2008 The force needed to move an atom on a surface *Science* **319** 1066–9

[135] Albers B J, Schwendemann T C, Baykara M Z, Pilet N, Liebmann M, Altman E I and Schwarz U D 2009 Three-dimensional imaging of short-range chemical forces with picometre resolution *Nat. Nanotechnol.* **4** 307–10

[136] Sweetman A, Rashid M A, Jarvis S P, Dunn J L, Rahe P and Moriarty P 2016 Visualizing the orientational dependence of an intermolecular potential *Nat. Commun.* **7** 10621

[137] Arunan E *et al* 2011 Defining the hydrogen bond: an account (IUPAC technical report) *Pure Appl. Chem.* **83** 1637–41